




Elucidating the complex hydrolysis and conversion network of xanthan-like extracellular heteropolysaccharides in waste activated sludge fermentation

Chen-Yuan Zhou^{a,1}, Kun Dai^{a,1}, Yi-Peng Lin^a, Xing-Chen Huang^a, Yan-Lin Hu^a, Xuan-Xin Chen^a, Xiao-Fei Yang^a, Qi-Yuan Sun^b, Yong Zhang^b, Mark C.M. van Loosdrecht^c, Raymond Jianxiong Zeng^{a,*}, Fang Zhang^{a,*} 

^a Center of Wastewater Resource Recovery, College of Resources and Environment, Fujian Agriculture and Forestry University, Fuzhou, Fujian 350002, China

^b College of Environmental Science and Engineering, Fujian Normal University, Fuzhou, Fujian 350007, China

^c Department of Biotechnology, Delft University of Technology, Julianalaan 67, Delft 2628 BC, the Netherlands

ARTICLE INFO

Keywords:

Xanthan-degrading consortium
Heteropolysaccharides
Degradation network
Xanthan lyase
Methane production

ABSTRACT

The hydrolysis of structural extracellular polymeric substances (St-EPS) is considered a major limiting step in the anaerobic fermentation of waste activated sludge (WAS). However, the degradation of heteropolysaccharides, characterized by complex monomers of uronic acids and neutral saccharides in St-EPS, has rarely been reported. In this study, microbial-produced xanthan-like heteropolysaccharides, characterized by a blue filamentary film, were identified. The xanthan-producing bacteria comprised ~7.2% of total genera present in WAS. An xanthan-degrading consortium (XDC) was enriched in an anaerobic batch reactor. This consortium could degrade Xanthan for over 90% and disrupt the gel structure of xanthan while promoting methane production from WAS by 29%. The xanthan degradation network consisting of extracellular enzymes and bacteria was elucidated by combining high-throughput sequencing, metagenomic, and metaproteomic analyses. Five enzymes were identified as responsible for hydrolyzing xanthan to monomers, including xanthan lyase, β -D-glucosidase, β -D-glucanase, α -D-mannosidase, and unsaturated glucuronyl hydrolase. Seven genera, including *Paenibacillus* (0.2%) and *Clostridium* (3.1%), were identified as key bacteria excreting one to five of the aforementioned enzymes. This study thus provides insights into the complex conversions in anaerobic digestion of WAS and gives a foundation for future optimization of this process.

1. Introduction

Large quantities of waste activated sludge (WAS) are produced daily in wastewater treatment plants (WWTPs) (Hu et al., 2023). Anaerobic fermentation is an important biotechnology employed to recover CH₄ or volatile fatty acids (VFAs) from WAS (Wang et al., 2024a; Wen et al., 2025). The hydrolysis of complex components of the structural extracellular polymeric substances (St-EPS) is considered to be a major limiting step for the anaerobic fermentation of WAS (Guo et al., 2020; Li et al., 2024; Toja Ortega et al., 2022). Thermal and chemical pretreatment technologies have been proposed to enhance St-EPS hydrolysis, but these methods release recalcitrant unwanted organics and increase the treatment cost (Elalami et al., 2020; Sanawar et al., 2018; Wang et al., 2022). Enzymatic pretreatment (e.g. by α -amylase and protease)

has been suggested as a pretreatment method with highly selective and moderate reasons (Teo and Wong, 2014; Toja Ortega et al., 2022; Zhang et al., 2023). However, in general, limited enzymatic hydrolysis is observed, likely due to the instability of free enzymes, but also due to the complex nature of the St-EPS (Lü et al., 2016; Teo and Wong, 2014). Enhancing the natural capacity of hydrolytic bacteria would be a more preferred and elegant option to enhance WAS digestion.

Several biomolecular and chemical methods were developed in recent decades to identify and characterize the key gelling components in St-EPS (Bolej et al., 2020; 2018). Hydrolyzed St-EPS was found to contain more than 10 monomers, including neutral sugars, uronic acids, and amino sugars (Felz et al., 2019; Hu et al., 2023), while these can be connected by different types of bondings. The study of degradation of polysaccharides is typically focused on homopolysaccharides with a

* Corresponding author.

E-mail address: zhfang@mail.ustc.edu.cn (F. Zhang).

¹ C.-Y. Z. and K. D. contributed equally to this work.

single glycosidic bond, such as dextran and chitin (Geng et al., 2021; Lu et al., 2023; Zhang et al., 2021). In such cases, a single enzyme is typically sufficient for the hydrolysis of the homopolysaccharides. While, the hydrolysis and subsequent acidogenesis process of heteropolysaccharides, comprising complex monomers of uronic acids and neutral saccharides via multiple glycosidic bonds, will necessitate the participation of multiple bacteria and a wide suite of hydrolytic exoenzymes. For example, xanthan is a natural microbial extracellular heteropolysaccharide produced by *Xanthomonas campestris* (Dueholm et al., 2023; Vorhölter et al., 2008). Dueholm et al. (2023) detected the gene clusters for xanthan production in WAS, but the potential producers were not identified. The structure of xanthan represents

repeating pentasaccharide units of glucose, mannose, and glucuronate in a ratio of 2:2:1, which form a β -glucan backbone of β -1,4-glycosidic bonds and side chains of (α -1,3)-mannose-(β -1,4)-glucuronate-(β -1,2)-mannose (Fig. S1). However, the role of xanthan-degradation in anaerobic fermentation of St-EPS and WAS has not yet been the subject of previous studies, to the best of our knowledge.

The degradation of xanthan was mainly reported under aerobic conditions. For example, *Paenibacillus alginolyticus*, was isolated as xanthan degrading organism from the soil, but just degraded ~28% of xanthan due to the poor degradation of the β -glucan backbone (Ruijsenaars et al., 1999). The degradation of xanthan necessitates the involvement of multiple excreted enzymes, such as xanthan lyase (EC

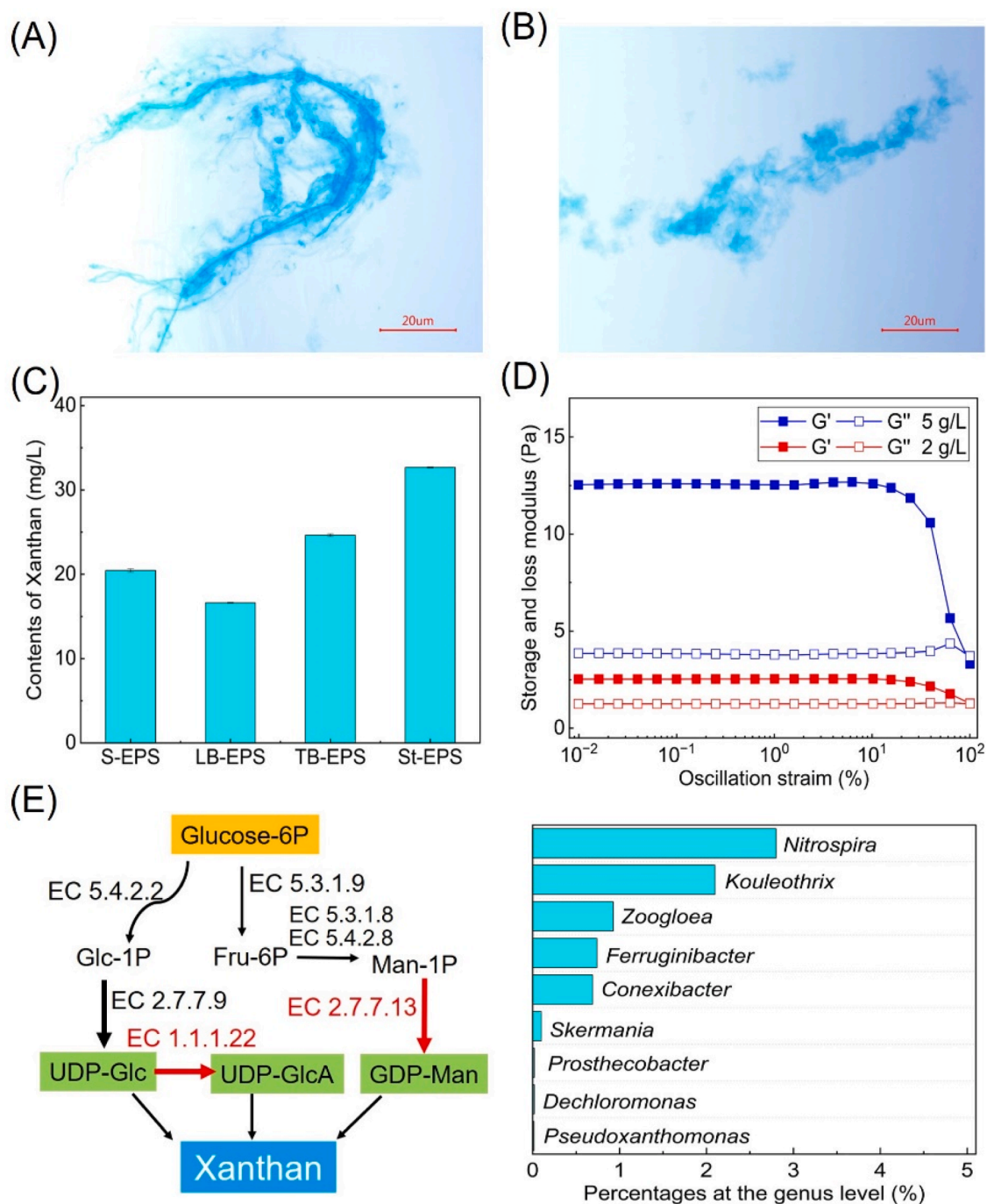


Fig. 1. Identifying xanthan-like heteropolysaccharides in WAS. (A) xanthan and (B) St-EPS dyeing by Alcian blue, (C) xanthan contents in EPS samples, (D) storage and loss moduli by the strain sweep, (E) xanthan producers identified in WAS.

4.2.2.12) and β -D-glucanase (EC 3.2.1.91), which are likely produced by different bacteria. An enrichment culture is therefore more suited to study the degradation of xanthan. A combination of multiple methods, including chemical analysis, high-throughput sequencing, and

metagenomic analysis, may provide reliable insights into the complex network of degradation and metabolic processes occurring within the mixed culture (Bolejic et al., 2018; de Bruin et al., 2022; Yu, 2020).

Thus, this study aimed to reveal the occurrence of xanthan-like

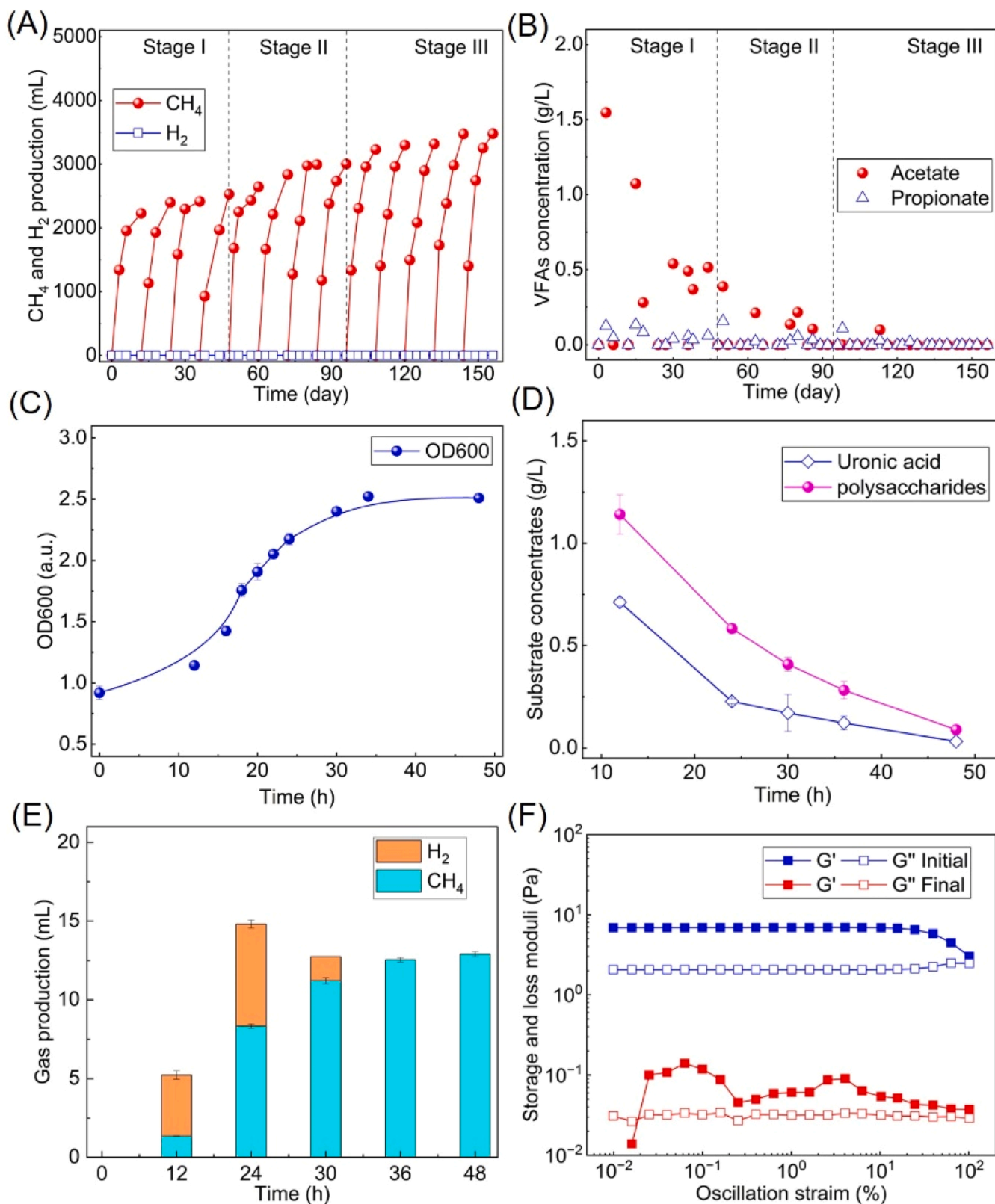


Fig. 2. Enrichment of xanthan-degrading consortium in a mesophilic reactor. (A) methane production in a 150-day operation, (B) acetate and propionate concentrations, (C) growth curve, (D) substrate conversion, (E) gas production, and (F) storage and loss moduli.

heteropolysaccharides in WAS and demonstrate the degradation network and metabolic conversions by the enriched xanthan-degrading consortium (XDC). It was anticipated that the enrichment culture of XDC would enhance WAS fermentation. The combined use of high-throughput sequencing, metagenomic, and metaproteomic analyses enabled the identification of both extracellular enzymes and key bacteria. Based on the aforementioned results, a degradation network was constructed and the metabolic relations were revealed. The findings will provide a good foundation for revealing the mechanism of heteropolysaccharides degradation and the enriched culture might serve as a new option to improve WAS fermentation.

2. Results and discussion

2.1. Occurrence of xanthan-like heteropolysaccharides in WAS

The content of St-EPS in this study was 37.9 ± 4.3 mg/gVSS, which was consistent with former data of 40–100 mg/gVSS (Lin et al., 2013; Wang et al., 2024b). Xanthan is a typical exopolysaccharide containing monomers of neutral sugars such as mannose and glucose, as well as the uronic acid glucuronate, all of which were identified in the St-EPS hydrolysates of WAS (Felz et al., 2019; Hu et al., 2023). Fig. 1A and B show the blue filamentary film of xanthan and St-EPS extracted from WAS by dyeing with alcian blue. The concentrations of xanthan-like heteropolysaccharides in EPS were determined to be approximately 20 mg/L in slime EPS (S-EPS), loosely bound EPS (LB-EPS), and tightly bound EPS (TB-EPS) samples, whereas in St-EPS, the concentration increased to 32 mg/L (Fig. 1C). The profiles of storage and loss moduli from the strain sweep indicated the gel-like properties of xanthan (Fig. 1D), and increasing the xanthan concentration from 2 to 5 g/L further enhanced the storage modulus, apparent viscosity, and compliance (Fig. S1).

The exopolysaccharide presence in WWTPs depends on the involved microorganisms (Weissbrodt et al., 2013). The genera *Bacteriodes* (12.61%), *norank_f_PHOS-HE36* (4.45%), and *norank_f_Saprosiraceae* (4.25%) were identified as the dominant bacteria in WAS (Fig. S2 and Table S2). *Xanthomonas*, *Stenotrophomonas*, *Xylella*, and *Pseudoxanthomonas* are closely related genera to produce xanthan in the family Lysobacteraceae (Timilsina et al., 2020). Interestingly, *Pseudoxanthomonas* (0.014%) was also identified in this work. Fig. 1E shows three typical precursors to produce xanthan, including UDP-glucose, UDP-glucuronic acid, and UDP-mannose, which are produced via the key enzymes UDP-glucose pyrophosphorylase (EC 2.7.7.9), UDP-glucose 6-dehydrogenase (EC 1.1.1.22), and GDP-mannose pyrophosphorylase (EC 2.7.7.13), respectively. All enzymes in Fig. 1E are encoded in WAS (Figs. S3 and S4). Fig. 1E summarizes that approximately 7.4% of bacteria, including *Nitrospira* (2.8%), *Kouleothrix* (2.1%), and *Zoogloea* (0.93%), were identified as xanthan-like heteropolysaccharides producers (Tables S3 and S4). Thus, Fig. 1 collectively demonstrates the occurrence of xanthan-like heteropolysaccharides in WAS.

2.2. Enrichment of a xanthan-degrading consortium and the growth curve

Fig. 2A shows that methane was the primary gaseous metabolite of xanthan over more than 150 days of operation, and no hydrogen was detected. 1/3 of the medium was replaced at the end of stage I (Day 48) and stage II (Day 96) to enhance the activity of enriched XDC. Indeed, the final yields increased from 2643 mL in stage I to 3480 mL in stage III. Fig. 2B shows that in stage III no VFAs were detected at the end of each cycle. The final concentration of biomass on Day 150 was 2.2 g/L (Fig. S5). The COD recovery in Stage III as methane was $78.7 \pm 2.3\%$ ($n = 4$) of xanthan added. When considering an anaerobic biomass COD yield on xanthan of 8–18% (Zhang et al., 2019), the COD balance closed reasonably well in this study.

Fig. 2C and D reveal the activity of enriched anaerobic XDC, the OD600 increased from 0.92 ± 0.06 to 2.5 ± 0.2 within 48 h and the uronic acids and polysaccharides decreased in 48 h to below 0.3 g/L.

Methane and hydrogen were detected in the headspace, but hydrogen was converted to methane eventually (Fig. 2E). Acetate (1.3 ± 0.01 g/L) and propionate (0.2 ± 0.003 g/L) were the main metabolites (Fig. S5). pH values did not decrease much (data not shown). The lower values of storage and loss moduli (Fig. 2F), apparent viscosity, and compliance (Fig. S5) indicated the damage to the xanthan gel structure after anaerobic degradation. These results all supported a good activity of enriched XDC.

2.3. Enhanced production of methane from WAS by the enriched XDC

Fig. 3A shows that the methane production reached 57.4 ± 1.2 mL on Day 30 in the WAS group, with no hydrogen detected. Methane production increased significantly by 29.3% to 74.2 ± 3.6 mL after the addition of XDC to WAS. The main intermediates (~ 0.2 g/L) were acetate and propionate in WAS fermentation, with minor quantities (< 0.09 g/L) of i-butyrate and n-butyrate also detected. These were completely consumed by Day 21 (Fig. 3B). After dosing with XDC in WAS (Fig. S6), propionate was detected as the only intermediate on Day 3 (0.06 g/L). Fig. 3C shows that St-EPS could be utilized by the enriched XDC and the final methane production was 12.6 mL. While, VFAs were undetected during the 30-d operation (Fig. S6), which was attributed to the elevated metabolic activity of XDC.

Glucuronate, mannose, and β -glucan are typical components of xanthan and St-EPS, therefore, the degradation of these organics by enriched XDC was further investigated. For glucuronate, the accumulated methane reached 30.7 ± 0.03 mL on Day 12 and did not increase much in the following days (Fig. 3D), and no H_2 was detected. Accumulated VFAs were consumed after Day 9 (Fig. S6). The methane production from mannose was 36.0 ± 2.9 mL, after Day 6, acetate and propionate were all undetected (Fig. S6). Interestingly, the β -glucan backbone, hindering the degradation of xanthan by *Paenibacillus algolyticus* XL-1 (Ruijsenaars et al., 1999), could be rapidly consumed by the enriched XDC. The methane production was 31.8 ± 0.6 mL on Day 15 and did not increase much in the following days (Fig. 3D). The concentration of accumulated propionate was just 0.15 g/L on Day 3 (Fig. S6). Thus, besides xanthan-like heteropolysaccharides and St-EPS, the enriched XDC could rapidly degrade the organics in WAS and promote methane production, demonstrating the advantage of mixed culture fermentation over pure culture fermentation.

2.4. Identification of extracellular enzymes in XDC for the xanthan hydrolysis

Five distinct enzymes involved in the depolymerization of xanthan were identified in the aerobically grown *Bacillus* sp. strain *GL1*, including xanthan lyase (EC 4.2.2.12), β -D-glucanase (EC 3.2.1.91), β -D-glucosidase (EC 3.2.1.21), unsaturated glucuronyl hydrolase (EC 3.2.1.180), α -D-mannosidase (EC 3.2.1.24) (Berezina et al., 2024; Nankai et al., 1999). Fig. 4A shows that for the xanthan lyase in enriched XDC, the absorbance at $UV_{235\text{ nm}}$ increased 1.1 ± 0.05 after 4 h, which was significantly higher than that of WAS (< 0.02). The activity value was 10.6 ± 0.08 mU/mL, which was comparable to that of *Bacillus* sp. strain *GL1* ($1.7 - 15.6$ mU/mL) (Ruijsenaars et al., 1999). Fig. 4B shows that the activity of β -D-glucanase and α -D-mannosidase in XDC was 64.1 ± 3.1 U and 4.3 ± 0.05 mU, respectively, which were all higher than those observed for WAS (5.3 ± 0.8 U and 1.5 ± 0.06 mU).

Fig. 4C illustrates the detection of multiple protein bands ranging from 10 to 130 kDa via SDS-PAGE. In this study, five above enzymes (Figs. 4D and S7, and Table S5) were all identified with high similarities (from 33.6% to 96.3%) and low e-values (from 0 to $1e^{-55}$), including XDC_k97_244,882_3_1 for xanthan lyase, XDC_k97_113,972_1_1 for β -D-glucanase, XDC_k97_15,684_2_1 for β -D-glucosidase, XDC_k97_46,018_10_1 for unsaturated glucuronyl hydrolase, and XDC_k97_87,739_40_1 for α -D-mannosidase, respectively. Except for xanthan lyase (not available in the SWISS-MODEL database), the 3D-

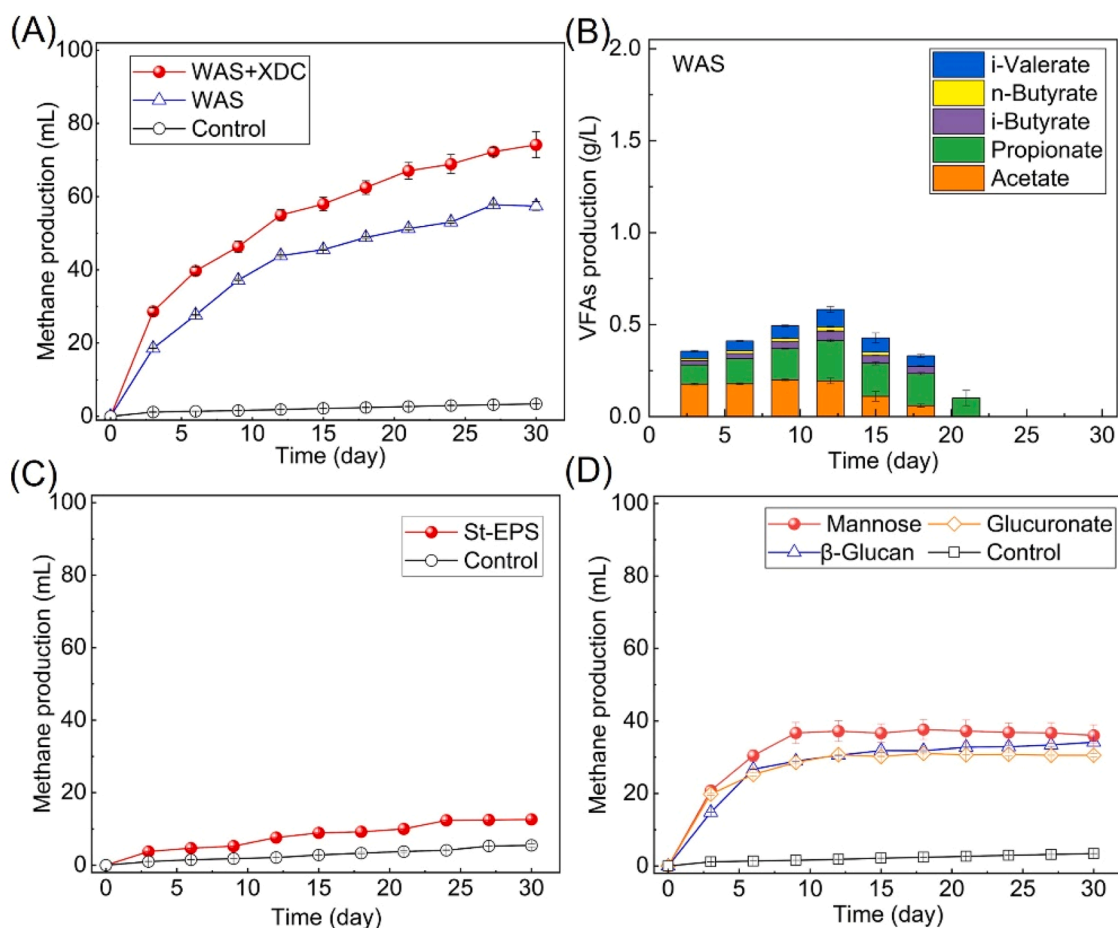


Fig. 3. Methane production from WAS by the enriched XDC. (A) Methane and (B) VFAs production from WAS, (C) methane production from St-EPS, and (D) methane production from typical organics.

structures of the other four enzymes were finally constructed (Fig. 4E), respectively. These data all supported the enhanced hydrolytic capacity of XDC, which facilitated the hydrolysis of xanthan into monomers of glucose, mannose, and unsaturated glucuronate.

2.5. Diversity and metabolic pathway of xanthan in the enriched XDC

The microbial diversity analysis (Figs. 5A, S8, and Table S6) indicated that the bacterial composition in the enriched XDC was > 90% at the domain level (Fig. S8). The top 30 enriched genera are summarized in Fig. 5A, with the main genera being *Thermovirga*, *DMER64*, and *Proteiniphilum*. The relative abundance of *Thermovirga* remained relatively stable, ranging from 20.6% to 23.6%. In contrast, the relative abundance of *DMER64* increased from 7.2% in XDC20 to 27.9% in XDC150, while *Proteiniphilum* increased from 10.7% in XDC20 to 17.0% in XDC150. The genus *Thermovirga* is an isolated amino-acid-degrading bacterium that primarily utilizes proteinous substrates (Dahle and Birkeland, 2006). *Proteiniphilum saccharofermentans*, isolated from a mesophilic laboratory-scale biogas reactor (Tomazetto et al., 2018). However, the function of xanthan degradation by these genera was hitherto unknown. Interestingly, a xanthan-degrading genus of *Paenibacillus* was also identified, but the percentage was just 0.2% in XDC150. The xanthan-producing bacteria in WAS were all undetected in XDC150.

The metabolic pathway of xanthan degradation was further investigated by combining metagenomic and metaproteomic analyses. Extracellular enzymes of xanthan lyase, β -D-glucanase, β -D-glucosidase, unsaturated glucuronyl hydrolase, α -D-mannosidase were all encoded in the XDC metagenome (Fig. 5B). Over 40 genera in the enriched XDC

were identified in Tables S7–S11. Seven key bacteria with a percentage above 0.01% are summarized in Fig. 5B, including *Paenibacillus* (0.2%), *Clostridium* (3.1%), *Proteiniphilum* (17.0%), *Petrimonas* (0.6%), *Mesotoga* (4.9%), *Ornatilinea* (0.02%), *Leptolinea* (0.03%). Of which, *Paenibacillus* (0.2%) was identified as capable of producing all five enzymes. The remaining six genera just excreted one to four of the aforementioned enzymes, for example, *Clostridium* exhibited the potential for two enzymes, namely xanthan lyase and β -D-glucosidase. *Paenibacillus algino-lyticus* XL-1 can degrade ~28% of xanthan (Ruijsenaars et al., 1999). The percentages of these seven genera in WAS were all below 0.01% (Fig. 1), indicating a higher XDC activity on the enhanced degradation of xanthan-like heteropolysaccharides in WAS (Fig. 3).

Finally, the produced three monomers of xanthan, including unsaturated glucuronate, mannose, and glucose, were then converted to pyruvate via the typical enzymes in the modified Entner-Doudoroff and Embden-Meyerhof-Parnas pathways (Figs. 5C and S9–14). Acetate, propionate, butyrate, and methane were the final products of pyruvate by the anaerobes in the enriched XDC. Fig. 5D further shows that the relative abundances of identified specific enzymes in XDC were higher than that of WAS, supporting the high activity of XDC on xanthan hydrolysis (Fig. 4), EPS degrading, and metabolites production (Fig. 3). Lastly, two archaeal genera *Methanobacterium* (8.9%) and *Methanosaeta* (1.8%) were also enriched in XDC150 these can convert hydrogen and acetate to methane, which was consistent with CH_4 production from xanthan in Figs. 2 and 3.

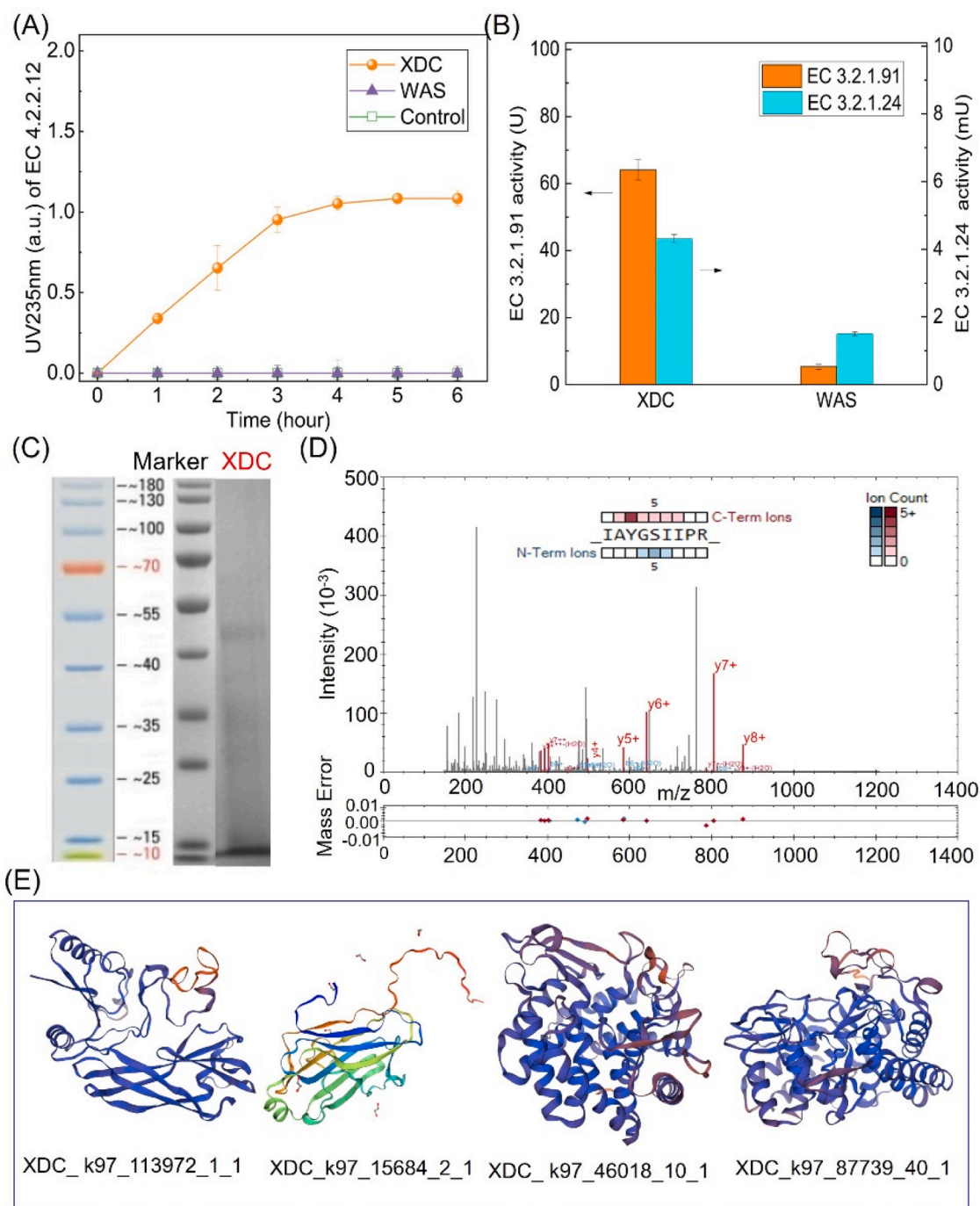


Fig. 4. Identification of extracellular enzymes for xanthan hydrolysis by metaproteomics analysis and SWISS-MODEL. Activities (A) xanthan lyase and (B) β -D-glucanase and α -D-mannosidase, (C) SDS-PAGE bands, (D) MS² spectrum of identified peptide in XDC_k97_244,882_3_1, (E) 3D-structure of four enzymes.

2.6. Role of degradation network on xanthan fermentation and environmental implication

The hydrolyzed St-EPS was found to contain over 10 monomers, including neutral sugars, uronic acids, and amino sugars (Felz et al., 2019; Hu et al., 2023). This study elucidated, for the first time, that the degradation network of xanthan was composed of five hydrolases and seven key genera within the enriched XDC (Fig. 5). Notably, the genus *Paenibacillus* (0.2%) was identified as capable of excreting all five enzymes necessary for xanthan hydrolysis, suggesting that this genus can utilize xanthan independently. However, the intact xanthan backbone was found to limit its degradation by *Paenibacillus alginolyticus* XL-1

(Ruijsenaars et al., 1999). Furthermore, the genus *Clostridium* was also capable of excreting xanthan lyase (EC 4.2.2.12), with a relative abundance of 3.1%, which was higher than that of *Paenibacillus* (0.2%). Berezina et al. (2024) also reported that the *Clostridium* genus entailed the enzymatic depolymerization of xanthan via the highly specialized xanthan lyase. Other genera of *Clostridium*, *Petrimonas* (0.6%), *Mesotoga* (4.9%), *Ornatilinea* (0.02%), *Leptolinea* (0.03%) can excrete enzymes of β -D-glucanase (EC 3.2.1.91) and β -D-glucosidase (EC 3.2.1.21) to break the backbone of β -glucan structure. A high percentage of *Proteiniphilum* (17.0%) in XDC was capable of excreting enzymes EC 3.2.1.180 and EC 3.2.1.24, which convert the released oligosaccharides into xanthan monomers. In short, the degradation network formed by the mixed

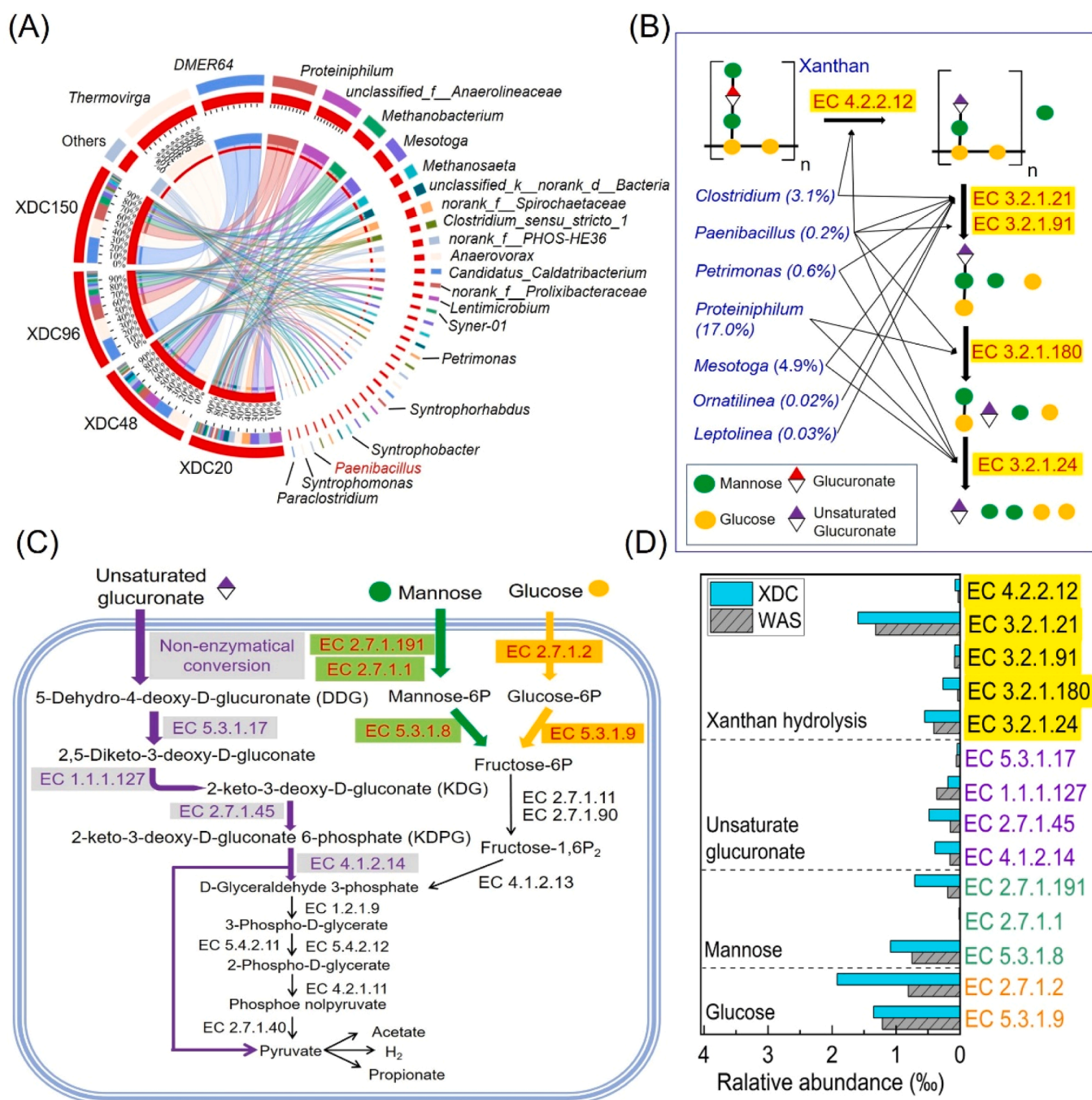


Fig. 5. Diversity and xanthan metabolism in the enriched XDC. (A) bacterial diversity at the genus level, (B) extracellular enzymatic pathway, (C) metabolic pathway of xanthan hydrolysates, (D) relative abundance of key genes.

culture exhibits a distinct advantage in terms of xanthan degradation over pure culture, which is in accordance with the experimental data on substrate utilization (almost 100%) and metabolite production, as illustrated in Figs. 2–4.

Recently, Geng et al. (2021) enriched a *Bacteroides*-dominated anaerobic consortium to promote methane production from WAS via the excretion of alginate lyase (EC 4.2.2.3). Lapébie et al. (2019) reported that *Bacteroidetes* use thousands of enzyme combinations to break down polysaccharides. Thus, it can be postulated that, besides alginate lyase (EC 4.2.2.3), other enzymes in *Bacteroidetes* and enriched bacteria may also be involved in the degradation network of organics to produce methane. It is also important to note that the percentage of xanthan-degrading bacteria observed in this study was relatively low.

Zhuang et al. (2022) reported that the *DMER64* genus could convert cellulose to acetate via excreting β -glucosidase (EC 3.2.2.21), however, we did not identify the same function in this work. The continuously stirred tank reactor is known as a valid tool to remove low-activity bacteria and enrich high-activity bacteria (Dai et al., 2020), which will be carried out in the future to reveal the xanthan metabolism of enriched XDC. In general, this work offers a useful framework for examining the degradation mechanism of unacquainted heteropolysaccharides in WAS.

Besides the organic compounds, the presence of multivalent metal ions (e.g., Ca²⁺ and Mg²⁺) may play structural skeletal functions (Dueholm et al., 2023; Lin et al., 2017), thus restricting the degradation of xanthan and EPS in WAS. After removing divalent cations in WAS,

XDC would enhance a higher methane production, which will be investigated in the future. Meanwhile, since xanthan is widely used as a gelling and stabilizing agent in the food and oil industries (Wang et al., 2017), the xanthan-like heteropolysaccharides may also be excreted from WAS and used as valuable materials. However, the excreting and purifying method should be developed since kinds of gelling organics are excreted from WAS by the heat- Na_2CO_3 method.

3. Conclusions

This study demonstrated the occurrence of xanthan-like heteropolysaccharides in WAS, revealing that xanthan-producing bacteria comprise approximately 7.2% of the total genera in WAS. The enriched XDC exhibited an unexpectedly high degree of degradation (>90%), which could promote CH_4 production by 29% via the disruption of the WAS gel structure. The multi-omics analysis revealed a degradation network involving five extracellular enzymes and seven genera. The identification of five extracellular enzymes (i.e. xanthan lyase, β -D-glucanase, β -D-glucosidase, unsaturated glucuronyl hydrolase, and α -D-mannosidase) capable of hydrolyzing xanthan to monomers was a key finding of the study. The presence of seven genera, including *Paenibacillus* (0.2%) and *Clostridium* (3.1%), was identified in the enriched XDC, thereby facilitating the degradation of xanthan. These advancements have led to a more profound comprehension of the pivotal role played by heteropolysaccharides in WAS fermentation.

4. Materials and methods

4.1. Inocula and enrichment of a xanthan-degrading consortium

The inoculum was a mixture of collected WAS (Jinshan wastewater treatment plant, Fuzhou, China) and mesophilic anaerobic sludge (Wang et al., 2022). Table S1 shows the parameters of WAS, such as pH and SCOD. A mesophilic (35 °C) batch reactor was constructed with a working volume of 2.2 L and VSS of 4 g/L. 5 g/L of xanthan was added every 12 days to enrich the XDC. 1/3 of the inorganic medium (Zhang et al., 2019) was replaced at the end of stage I (Day 48) and stage II (Day 96) to enhance the activity of enriched XDC. The pH was maintained at 7.0 ± 0.2 by adding 1 M NaOH or HCl as needed.

4.2. Activities of enriched XDC and excreted extracellular enzymes

To evaluate the activity of enriched XDC, the growth curve was determined in a thermostatic shaker at 35 °C. The biomass (5 mL) xanthan (5 g/L), and inorganic medium (55 mL) were added to 120 mL serum bottles ($n = 3$). The OD_{600} values, uronic acids, polysaccharides, produced CH_4 , H_2 , and VFAs were all determined. The extracellular enzymes were collected from the XDC supernatant. Inorganic medium (30 mL), xanthan (2 g/L), and enzymes (30 mL) were added into 120 mL serum bottles ($n = 3$) and incubated under pH 7.0 and 35 °C. The activity of xanthan lyase (EC 4.2.2.12) was determined based on the change in absorbance at $\text{UV}_{235\text{nm}}$. The supernatant of WAS was also collected and named as the WAS group. Moreover, the extracellular enzymatic activities of β -D-glucanase (EC 3.2.1.91) and α -D-mannosidase (EC 3.2.1.24) in WAS and XDC groups were also determined using two available kits of glucanase and mannosidase, respectively.

4.3. WAS fermentation by dosing with XDC

The collected WAS was subsequently used to evaluate methane production by dosing with XDC. The enriched XDC (120 mL) was centrifuged to remove broth. In the WAS+XDC group, 50 mL of WAS, 10 mL of inorganic medium, and 10 mL of collected XDC (at a ratio of 0.2 g VSS/g VSS to WAS) were added into 120 mL serum bottles ($n = 3$). In the control group ($n = 3$), no WAS was added. While no XDC was added in the WAS group ($n = 3$). The three groups were incubated under 35 °C

and pH 7.0 in the same shaker.

4.4. Degradation of St-EPS and typical carbohydrates by enriched XDC

St-EPS was extracted from the collected WAS (150 mL) by the heat- Na_2CO_3 method (Felz et al., 2016) was diluted with inorganic medium to 150 mL. The enriched XDC (60 mL) was collected to remove broth. In the St-EPS group, 50 mL St-EPS, 10 mL inorganic medium, and collected XDC (20 mL) were added into serum bottles ($n = 3$). No St-EPS was added in the control group ($n = 3$). These groups were incubated under 35 °C and pH 7.0 in a shaker at 120 rpm. As typical components of xanthan, glucuronate, mannose, and β -glucan are also the components in St-EPS (Hu et al., 2023). Thus, the degradation of these organics (2 g/L, $n = 3$) by enriched XDC (10 mL) in 120 serum bottles under 35 °C and pH 7.0 was further investigated in the same shaker. The control group ($n = 3$) was also constructed without dosing substrates.

4.5. Analysis

St-EPS was extracted from WAS by the heat- Na_2CO_3 method (Felz et al., 2016), and S-, LB-, and TB-EPS were also extracted from WAS by the heat method (Li and Yang, 2007). The contents of xanthan-like heteropolysaccharides in St-EPS, S-, LB-, and TB-EPS were determined using Alcian blue as a probe under $\text{UV}_{787\text{nm}}$ (Passow and Aalredge, 1995). The morphology of xanthan and xanthan-like heteropolysaccharides in WAS was analyzed via an optical microscope (BX43, Olympus, China). The activity of xanthan lyase was determined at $\text{UV}_{235\text{nm}}$ by a UV-visible spectrophotometer (A560, AOE Instruments, China). The enzymatic activities of β -D-glucanase and α -D-mannosidase were determined using two commercially available kits for glucanase and mannosidase (Solarbio, Beijing, China). The concentration of uronic acid was determined by the carbazole-sulfuric acid method. The concentrations of ethanol and VFAs were quantified by a 7890 gas chromatography (Agilent, United States). The contents of CH_4 and H_2 were determined with a SP7890 gas chromatograph (Lunan, China). The rheological properties were evaluated using a rheometer (MCR 301, Anton Paar Physica, Austria).

4.6. Hydrolases, microbial diversity, and metabolic pathway

Five DNA samples were extracted from the WAS and XDC reactor on Days 20, 48, 96, and 150, respectively, and labelled as WAS, XDC20, XDC48, XDC96, and XDC150, respectively. Sequencing using primers of 341F-806R (Zhang et al., 2019) was subsequently conducted on the Illumina MiSeq PE 300 sequencer. The raw reads were analyzed in the Majorbio platform (Ren et al., 2022). The extracellular enzyme of XDC was visualized via SDS-PAGE analysis. Then, protein components for metaproteomic analysis were analyzed by LC-MS/MS (Thermo Fisher, Germany) and processed in NCBI and UniProt databases. The structures of identified enzymes were then built using the SWISS-MODEL. WAS and the enriched XDC150 were ultimately sequenced by metagenomic analysis in the Novaseq 6000 platform (Majorbio, China). By combining the CAZY database and KEGG annotation, the pathway and the encoded enzymes were finally identified (Han et al., 2024).

CRedit authorship contribution statement

Chen-Yuan Zhou: Writing – original draft, Visualization, Validation, Investigation, Formal analysis, Data curation. **Kun Dai:** Writing – review & editing, Writing – original draft, Validation, Methodology, Investigation, Formal analysis, Data curation. **Yi-Peng Lin:** Visualization, Methodology, Investigation, Data curation. **Xing-Chen Huang:** Visualization, Validation, Methodology, Investigation, Data curation. **Yan-Lin Hu:** Visualization, Validation, Investigation, Data curation. **Xuan-Xin Chen:** Visualization, Validation, Formal analysis, Data curation. **Xiao-Fei Yang:** Visualization, Data curation. **Qi-Yuan Sun:** Visualization,

Methodology, Data curation. **Yong Zhang:** Visualization, Methodology, Investigation, Data curation. **Mark C.M. van Loosdrecht:** Writing – review & editing, Writing – original draft, Visualization, Methodology. **Raymond Jianxiang Zeng:** Writing – review & editing, Writing – original draft, Visualization, Investigation, Conceptualization. **Fang Zhang:** Writing – review & editing, Writing – original draft, Supervision, Project administration, Methodology, Funding acquisition, Conceptualization.

Declaration of competing interest

The authors declare that they have no known competing financial interests or personal relationships that could have appeared to influence the work reported in this paper.

Acknowledgments

The authors would like to acknowledge the financial support from the National Natural Science Foundation of China (Grant no: 52370130 and 52170127), the Natural Science Foundation of Fujian Province for Distinguished Young Scholars (2023J06021).

Supplementary materials

Supplementary material associated with this article can be found, in the online version, at [doi:10.1016/j.wroa.2025.100303](https://doi.org/10.1016/j.wroa.2025.100303).

Data availability

Data will be made available on request.

References

- Berezina, O.V., Rykov, S.V., Schwarz, W.H., Liebl, W., 2024. Xanthan: enzymatic degradation and novel perspectives of applications. *Appl. Microbiol. Biotechnol.* 108 (1), 227.
- Boleij, M., Kleikamp, H., Pabst, M., Neu, T.R., van Loosdrecht, M.C.M., Lin, Y., 2020. Decorating the anammox house: sialic acids and sulfated glycosaminoglycans in the extracellular polymeric substances of anammox granular sludge. *Environ. Sci. Technol.* 54 (8), 5218–5226.
- Boleij, M., Pabst, M., Neu, T.R., van Loosdrecht, M.C.M., Lin, Y., 2018. Identification of glycoproteins isolated from extracellular polymeric substances of full-scale anammox granular sludge. *Environ. Sci. Technol.* 52 (22), 13127–13135.
- Dahle, H., Birkeland, N.K., 2006. *Thermovirga lienii* gen. nov., sp. nov., a novel moderately thermophilic, anaerobic, amino-acid-degrading bacterium isolated from a North Sea oil well. *Int. J. Syst. Evol. Microbiol.* 56 (7), 1539–1545.
- Dai, K., Zhang, W., Zeng, R.J., Zhang, F., 2020. Production of chemicals in thermophilic mixed culture fermentation: mechanism and strategy. *Crit. Rev. Environ. Sci. Technol.* 50 (1), 1–30.
- de Bruin, S., Vasquez-Cardenas, D., Sarbu, S.M., Meysman, F.J.R., Sousa, D.Z., van Loosdrecht, M.C.M., Lin, Y., 2022. Sulfated glycosaminoglycan-like polymers are present in an acidophilic biofilm from a sulfidic cave. *Sci. Total Environ.* 829, 154472.
- Dueholm, M.K.D., Besteman, M., Zeuner, E.J., Riisgaard-Jensen, M., Nielsen, M.E., Vestergaard, S.Z., Heidelbach, S., Bekker, N.S., Nielsen, P.H., 2023. Genetic potential for exopolysaccharide synthesis in activated sludge bacteria uncovered by genome-resolved metagenomics. *Water Res.* 229, 119485.
- Elalami, D., Monlau, F., Carrere, H., Abdelouahdi, K., Ouakroum, A., Zeroual, Y., Barakat, A., 2020. Effect of coupling alkaline pretreatment and sewage sludge co-digestion on methane production and fertilizer potential of digestate. *Sci. Total Environ.* 743, 140670.
- Felz, S., Al-Zuhairy, S., Aarstad, O.A., van Loosdrecht, M.C.M., Lin, Y.M., 2016. Extraction of structural extracellular polymeric substances from aerobic granular sludge. *JoVE* 115, e54534.
- Felz, S., Vermeulen, P., van Loosdrecht, M.C.M., Lin, Y.M., 2019. Chemical characterization methods for the analysis of structural extracellular polymeric substances (EPS). *Water Res.* 157, 201–208.
- Geng, Z.Q., Qian, D.K., Hu, Z.Y., Wang, S., Yan, Y., van Loosdrecht, M.C.M., Zeng, R.J., Zhang, F., 2021. Identification of extracellular key enzyme and intracellular metabolic pathway in alginate-degrading consortia via an integrated metaproteomic/metagenomic analysis. *Environ. Sci. Technol.* 55 (24), 16636–16645.
- Guo, H., Felz, S., Lin, Y., van Lier, J.B., de Kreuk, M., 2020. Structural extracellular polymeric substances determine the difference in digestibility between waste activated sludge and aerobic granules. *Water Res.* 181, 115924.
- Han, C., Shi, C., Liu, L., Han, J., Yang, Q., Wang, Y., Li, X., Fu, W., Gao, H., Huang, H., Zhang, X., Yu, K., 2024. Majorbio cloud 2024: update single-cell and multiomics workflows. *iMeta* 3 (4), e217.
- Hu, Z.Y., Lin, Y.P., Wang, Q.T., Zhang, Y.X., Tang, J., Hong, S.D., Dai, K., Wang, S., Lu, Y. Z., van Loosdrecht, M.C.M., Wu, J., Zeng, R.J., Zhang, F., 2023. Identification and degradation of structural extracellular polymeric substances in waste activated sludge via a polygalacturonate-degrading consortium. *Water Res.* 233, 119800.
- Lapébie, P., Lombard, V., Drula, E., Terrapon, N., Henrissat, B., 2019. Bacteroidetes use thousands of enzyme combinations to break down glycans. *Nat. Commun.* 10 (1), 2043.
- Li, J., Chen, Y., Qi, J., Zuo, X., Meng, F., 2024. Characterization of EPS subfractions from a mixed culture predominated by partial-denitrification functional bacteria. *Water Res.* X 24, 100250.
- Li, X.Y., Yang, S.F., 2007. Influence of loosely bound extracellular polymeric substances (EPS) on the flocculation, sedimentation and dewaterability of activated sludge. *Water Res.* 41 (5), 1022–1030.
- Lin, L., Li, R.H., Yang, Z.Y., Li, X.Y., 2017. Effect of coagulant on acidogenic fermentation of sludge from enhanced primary sedimentation for resource recovery: comparison between FeCl₃ and PACl. *Chem. Eng. J.* 325, 681–689.
- Lin, Y.M., Sharma, P.K., van Loosdrecht, M.C.M., 2013. The chemical and mechanical differences between alginate-like exopolysaccharides isolated from aerobic flocculent sludge and aerobic granular sludge. *Water Res.* 47 (1), 57–65.
- Lü, F., Wang, J., Shao, L., He, P., 2016. Enzyme disintegration with spatial resolution reveals different distributions of sludge extracellular polymer substances. *Biotechnol. Biofuels* 9 (1), 29.
- Lu, Q., He, D., Liu, X., Du, M., Xu, Q., Wang, D., 2023. 1-Butyl-3-methylimidazolium chloride affects anaerobic digestion through altering organics transformation, cell viability, and microbial community. *Environ. Sci. Technol.* 57 (8), 3145–3155.
- Nankai, H., Hashimoto, W., Miki, H., Kawai, S., Murata, K., 1999. Microbial system for polysaccharide depolymerization: enzymatic route for xanthan depolymerization by *Bacillus* sp. Strain GL1. *Appl. Environ. Microbiol.* 65 (6), 2520–2526.
- Passow, U., Alldredge, A.L., 1995. A dye-binding assay for the spectrophotometric measurement of transparent exopolymer particles (TEP). *Limnol. Oceanogr.* 40 (7), 1326–1335.
- Ren, Y., Yu, G., Shi, C., Liu, L., Guo, Q., Han, C., Zhang, D., Zhang, L., Liu, B., Gao, H., Zeng, J., Zhou, Y., Qiu, Y., Wei, J., Luo, Y., Zhu, F., Li, X., Wu, Q., Li, B., Fu, W., Tong, Y., Meng, J., Fang, Y., Dong, J., Feng, Y., Xie, S., Yang, Q., Yang, H., Wang, Y., Zhang, J., Gu, H., Xuan, H., Zou, G., Luo, C., Huang, L., Yang, B., Dong, Y., Zhao, J., Han, J., Zhang, X., Huang, H., 2022. Majorbio cloud: a one-stop, comprehensive bioinformatic platform for multiomics analyses. *iMeta* 1 (2), e12.
- Ruijsenaars, H.J., Bont, J.A.M.d., Hartmans, S., 1999. A pyruvated mannose-specific xanthan lyase involved in xanthan degradation by *Paenibacillus alginolyticus* XL-1. *Appl. Environ. Microbiol.* 65 (6), 2446–2452.
- Sanawar, H., Pintel, I., Farhat, N.M., Bucs, S.S., Zlopasa, J., Kruihof, J.C., Witkamp, G.J., van Loosdrecht, M.C.M., Vrouwenvelder, J.S., 2018. Enhanced biofilm solubilization by urea in reverse osmosis membrane systems. *Water Res.* X 1, 100004.
- Teo, C.W., Wong, P.C.Y., 2014. Enzyme augmentation of an anaerobic membrane bioreactor treating sewage containing organic particulates. *Water Res.* 48, 335–344.
- Timilsina, S., Potnis, N., Newberry, E.A., Liyanapathirana, P., Iruegas-Bocardo, F., White, F.F., Goss, E.M., Jones, J.B., 2020. *Xanthomonas* diversity, virulence and plant–pathogen interactions. *Nat. Rev. Microbiol.* 18 (8), 415–427.
- Toja Ortega, S., van den Berg, L., Pronk, M., de Kreuk, M.K., 2022. Hydrolysis capacity of different sized granules in a full-scale aerobic granular sludge (AGS) reactor. *Water Res.* X 16, 100151.
- Tomazetto, G., Hahnke, S., Wibberg, D., Pühler, A., Klocke, M., Schlüter, A., 2018. *Proteiniphilum saccharofermentans* str. M3/6T isolated from a laboratory biogas reactor is versatile in polysaccharide and oligopeptide utilization as deduced from genome-based metabolic reconstructions. *Biotechnol. Rep.* 18, e00254.
- Vorhölter, F.J., Schneiker, S., Goesmann, A., Krause, L., Bekel, T., Kaiser, O., Linke, B., Patschkowski, T., Rückert, C., Schmid, J., Sidhu, V.K., Sieber, V., Tauch, A., Watt, S. A., Weisshaar, B., Becker, A., Niehaus, K., Pühler, A., 2008. The genome of *Xanthomonas campestris* pv. *campestris* B100 and its use for the reconstruction of metabolic pathways involved in xanthan biosynthesis. *J. Biotechnol.* 134 (1), 33–45.
- Wang, S., Hu, Z.Y., Geng, Z.Q., Tian, Y.C., Ji, W.X., Li, W.T., Dai, K., Zeng, R.J., Zhang, F., 2022. Elucidating the production and inhibition of melanoidins products on anaerobic digestion after thermal-alkaline pretreatment. *J. Hazard. Mater.* 424, 127377.
- Wang, S., Zhu, X.M., Hong, S.D., Zheng, S.J., Wang, Y.B., Huang, X.C., Tian, Y.C., Li, W. T., Lu, Y.Z., Wu, J., Zeng, R.J., Dai, K., Zhang, F., 2024a. Unveiling the occurrence and non-negligible role of amino sugars in waste activated sludge fermentation by an enriched chitin-degradation consortium. *Environ. Sci. Technol.* 58 (4), 1966–1975.
- Wang, Y.B., Tang, J., Ran, D.D., Zhu, X.M., Zheng, S.J., Hong, S.D., Fu, S.F., van Loosdrecht, M.C.M., Zeng, R.J., Dai, K., Zhang, F., 2024b. Deciphering the dual roles of an alginate-based biodegradable flocculant in anaerobic fermentation of waste activated sludge: dewaterability and degradability. *Environ. Sci. Technol.* 58 (32), 14282–14292.
- Wang, Z., Wu, J., Zhu, L., Zhan, X., 2017. Characterization of xanthan gum produced from glycerol by a mutant strain *Xanthomonas campestris* CCTCC M2015714. *Carbohydr. Polym.* 157, 521–526.
- Weissbrodt, D.G., Neu, T.R., Kuhllicke, U., Rappaz, Y., Holliger, C., 2013. Assessment of bacterial and structural dynamics in aerobic granular biofilms. *Front. Microbiol.* 4, 175.
- Wen, H.Q., Chen, G.L., Li, Y.S., Tian, T., Pan, Y., Yu, H.Q., 2025. An inconvenient impact: unveiling the overlooked differences in crystalline forms of iron (hydro)oxides on anaerobic digestion. *Water Res.* X 26, 100286.

- Yu, H.Q., 2020. Molecular insights into extracellular polymeric substances in activated sludge. *Environ. Sci. Technol.* 54 (13), 7742–7750.
- Zhang, F., Qian, D.K., Geng, Z.Q., Dai, K., Zhang, W., van Loosdrecht, M.C.M., Zeng, R.J., 2021. Enhanced methane recovery from waste-activated sludge by alginate-degrading consortia: the overlooked role of alginate in extracellular polymeric substances. *Environ. Sci. Technol. Lett.* 8 (1), 86–91.
- Zhang, F., Zhang, W., Qian, D.K., Dai, K., van Loosdrecht, M.C.M., Zeng, R.J., 2019. Synergetic alginate conversion by a microbial consortium of hydrolytic bacteria and methanogens. *Water Res.* 163, 114892.
- Zhang, M., Yang, Y., Mou, H., Pan, A., Su, X., Chen, J., Lin, H., Sun, F., 2023. Enhanced methane yield in anaerobic digestion of waste activated sludge by combined pretreatment with fungal mash and free nitrous acid. *Bioresour. Technol.* 385, 129441.
- Zhuang, H., Amy Tan, G.Y., Jing, H., Lee, P.H., Lee, D.J., Leu, S.Y., 2022. Enhanced primary treatment for net energy production from sewage – The genetic clarification of substrate-acetate-methane pathway in anaerobic digestion. *Chem. Eng. J.* 431, 133416.